Ligands Rock & Roll: Stepwise Twisting of Two *cis*-Coordinated Lopsided N-Heterocycles in an Octahedral Bis(2-phenylazopyridine)–Ruthenium(II) Complex with Seven Atropisomers

Aldrik H. Velders,*[a, b] Anna C. G. Hotze,[a] and Jan Reedijk[a]

Abstract: ^{1}H NMR data of α-[Ru(azpy)$_2$(MeBim)$_2$](PF$_6$)$_2$ (azpy = 2-phenylazopyridine, MeBim = 1-methylbenzimidazole), **2**, revealed the presence of a total of seven atropisomers at −95 °C: three head-to-tail, HT, isomers (A, C, and D), and four head-to-head, HH, isomers which, due to the presence of an intrinsic C_2 axis in the α-[Ru(azpy)$_2$] moiety, are two sets of identical pairs (B/*B* and E/*E*). The NMR data of **2** represent a unique example of a coordination compound that shows a variable temperature (VT) behavior with more, well-defined steps of slow-to-fast exchange of its atropisomers. At 65 °C, all atropisomers are in fast exchange; on lowering the temperature the sharp signals first broaden (at room temperature) and consecutively split up into two sets of relatively sharp signals, in slow exchange, at about 0 °C (D, 40 %, and the coalesced signals of AB*B*CE*E*, 60 %). Upon further cooling, the set of peaks belonging to D remain sharp until the lowest recording temperatures. The signals of the other set of resonances, on the other hand, first broaden again and then separate into two sets of broad peaks (C/E/*E* and A) and one set of sharp peaks (B and *B* in fast exchange); on lowering the temperature even more, these signals broaden once again and finally, at −95 °C, are split up into a total of four sets of signal (A, B/*B*, C, and E/*E*). At low temperatures, ROESY experiments revealed that atropisomerization occurs through the synchronous rotation of both MeBim ligands in the interconversion of the two "identical" HH atropisomers B and *B*, as well as in the interconversion between C and E/*E*. The HH rotamers B/*B* furthermore exhibit a slow-to-fast exchange atropisomerization behavior that is observed independently from the other dynamic processes in this compound. The versatile *cis* bifunctional binding of the DNA model bases (MeBim ligands) in **2** parallels the observation of α-[Ru(azpy)$_2$Cl$_2$] which shows extraordinarly high cytotoxicity against tumor cell lines.

Keywords: atropisomerism · bioinorganic chemistry · DNA model bases · NMR spectroscopy · ruthenium

Introduction

Understanding the binding of molecules to metal compounds is of great importance in many areas of inorganic chemistry, including bioinorganic chemistry,[1] and in particular also in the field of biomedicinal chemistry for the coordination of metal-based drugs to biological target molecules.[2–4] The binding of the well-known antitumor drug *cis*-[PtCl$_2$(NH$_3$)$_2$] to two neighboring guanines of DNA is generally accepted to be the main interaction responsible for its antitumor activity.[5,6] The orientation and rotational behavior of *cis* bifunctional coordinated square-planar platinum(II) complexes with lopsided N-heterocycles, like guanine derivatives, have been extensively investigated since the late 1970s by Cramer,[7,8] and others,[9–14] and are now at an advanced stage of understanding.[15–17] All factors influencing the orientation and dynamic behavior of lopsided ligands on *cis*-coordinated octahedral complexes are not as thoroughly understood, yet. However, it is of considerable interest to understand the coordinative binding of biologically available N-heterocycles to six-coordinate complexes,[18] like rutheni-

[a] Dr. A. H. Velders, Dr. A. C. G. Hotze, Prof. Dr. J. Reedijk
Leiden Institute of Chemistry, Gorlaeus Laboratories
Leiden University, P.O. Box 9502
2300 RA Leiden (The Netherlands)
E-mail: a.velders@chem.leidenuniv.nl

[b] Dr. A. H. Velders
Current address:
Laboratory of Supramolecular Chemistry and Technology
MESA+ Institute for Nanotechnology, University of Twente
P.O. Box 217, 7500 AE Enschede (The Netherlands)
Fax: (+31) 53-489-4645
E-mail: a.h.velders@utwente.nl

Supporting information for this article is available on the WWW under http://www.chemeurj.org/ or from the author.

 DOI: 10.1002/chem.200400590

um compounds, of which several are currently under investigation for their promising antitumor properties.[19–23] ^{1}H NMR spectroscopy has been proven to be a powerful tool to study the rotational behavior of σ-bound ligands in square-planar four-coordinate metal complexes. To date, however, only in a few suitable octahedral systems have the orientation and dynamic properties of σ-bound N-heterocycles been studied, like dinuclear μ-oxorhenium(v) complexes,[24–26] and dichlororuthenium(II)–dmso complexes.[24,27–30] More recently, we have introduced ruthenium(II)–bis(bipyridine) complexes of the type *cis*-[Ru(bpy)$_2$(L)$_2$](PF$_6$)$_2$ of which the dynamic process of heterocyclic ligands (L) can be studied very well with different kinds of monodentate ligands, whilst the backbone consists of two static didentate ligands.[31–33] With phosphonite ligands, ruthenium(II)–bis(bipyridine) complexes also appear as appealing compounds for their photochromically induced atropisomerization processes.[34,35]

The *cis*-dichloro complex α-[Ru(azpy)$_2$Cl$_2$] (azpy = 2-phenylazopyridine) shows cytotoxicity to a series of tumor cell lines even higher than that of the well-known antitumor complexes cisplatin and 5-fluorouracil.[20] Interestingly, the isomeric complex β-[Ru(azpy)$_2$Cl$_2$] and the structurally related complex *cis*-[Ru(bpy)$_2$Cl$_2$] are significantly less cytotoxic.[20,36] The pronounced differences in biological activity of these three structurally similar complexes (see Supporting Information) and related complexes, offer an interesting opportunity to search for structure–activity relationships of antitumor-active ruthenium complexes.[37,38] As DNA is a likely target for this kind of metallodrug, we have started to systematically investigate the binding of DNA bases to these compounds.

From DNA binding studies it has been reported that the *cis*-[Ru(bpy)$_2$] moiety can bind to nucleobases monofunctionally,[36] as well as bifunctionally,[39,40] in the latter case resulting in DNA interstrand cross-linking. Correspondingly, on reaction of *cis*-[Ru(bpy)$_2$(H$_2$O)$_2$]$^{2+}$ with non-tethered guanine derivatives, monofunctional adducts have been observed,[41] and, only recently, also a bifunctional adduct.[42] Initial DNA binding studies with the β-[Ru(azpy)$_2$][43,44] and α-[Ru(azpy)$_2$] moieties,[44–47] show monofunctional adducts upon reaction with guanine or adenine derivatives, but bifunctional DNA binding cannot be excluded, yet. For complexes of the type *cis*-[Ru(bpy)$_2$], α- and β-[Ru(azpy)$_2$] being borderline complexes with respect to the stable *cis* bifunctional coordination to non-tethered purines, these studies prompted us to investigate this aspect using the model bases 1-methylimidazole, MeIm, and 1-methylbenzimidazole, MeBim.[31,32,44,48] 1-Methyl(benz)imidazole derivatives are useful DNA model bases in the investigation of the bifunctional binding of sterically encumbered octahedral complexes,[18,24–30] and MeIm and MeBim form stable bisadducts with ruthenium bis(didentate) complexes. The imidazole H(ii) proton is structurally related to the H(8) atom of guanine derivatives, in addition, MeIm and MeBim possess a proton on the other side of the ligand, that is, H(iv), a most valuable (NMR) probe proton that is lacking in guanine derivatives (Scheme 1). The presence of the H(ii) and H(iv) protons appears to be fundamental for the unambiguous determination of the orientation and rotational behavior of the ligands on the ruthenium ion.

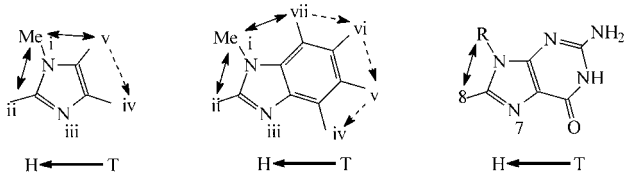

Scheme 1. Structural representation of MeIm, MeBim, and a (9*R*) guanine derivative, with the (^{1}H NMR) numbering scheme used and NOE (solid lines) and COSY (dashed lines) connectivities. The arrows below the structures, as used in Scheme 3, indicate the head and tail sites of the bases.

For the *cis*-[Ru(bpy)$_2$(MeBim)$_2$](PF$_6$)$_2$ complex, four atropisomers (three geometrically different ones) have been identified in solution using 1D and 2D ^{1}H NMR data.[31,32] In the β-[Ru(azpy)$_2$(MeBim)$_2$](PF$_6$)$_2$ complex on the other hand, only one conformer was observed and characterized.[44,48] We present here the synthesis, characterization, and variable temperature (VT) ^{1}H NMR behavior of the complexes α-[Ru(azpy)$_2$(MeIm)$_2$](PF$_6$)$_2$, **1**, and α-[Ru(azpy)$_2$(MeBim)$_2$](PF$_6$)$_2$, **2** (Scheme 2). The atropisomerization

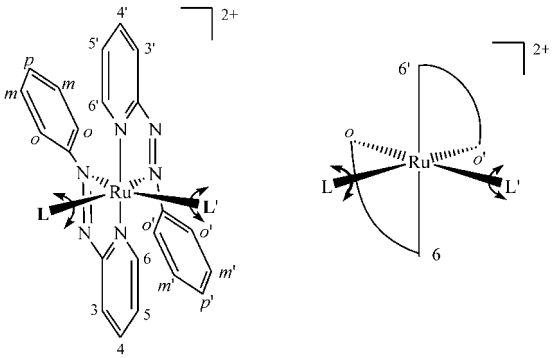

Scheme 2. Structural (left) and schematic (right) representation of the cation of (the Λ enantiomer of) α-[Ru(azpy)$_2$(L)$_2$](PF$_6$)$_2$ (L = MeIm for **1**; L = MeBim for **2**) and the proton numbering of the azpy ligands as used in the ^{1}H NMR discussions.

mechanism of **2** is unique and most peculiar: a total of seven atropisomers was observed (from which five are geometrically different), and the freezing out of the atropisomers occured in three well-observable steps, an as yet unprecedented phenomenon for rotational behavior of metal-coordinated molecules, which permits a close investigation of the atropisomerization processes of these kinds of complexes.

Results and Discussion

General: The ligand azpy lacks C_2 symmetry, so ruthenium(II)–bis(azpy) complexes of the type $[Ru(azpy)_2(X)_2]$ (in which X is a monodentate ligand, for example, Cl^-, H_2O, or NO_3^-) can occur as three *cis*-X and two *trans*-X isomers.[38,49] The α-isomer (with the pyridine molecules in a *trans* and the aza-nitrogen atoms in a *cis* geometry), is generally accepted to be the most stable isomer.[49–51] However, on extensive heating, or in substitution reactions of one of the monodentate ligands X in α-$[Ru(azpy)_2(X)_2]$ with incoming ligands (L), isomerization cannot be excluded.[52] In fact, in the reaction of α-$[Ru(azpy)_2(NO_3)_2]$ with guanine derivatives under refluxing conditions in water, three monofunctional adducts of the type $[Ru(azpy)_2(L)X]^+$ were formed: one α- and two β-isomers.[44,45] In the presented synthesis of **1** and **2**, the bisadducts of complexes of type α-$[Ru(azpy)_2(L)_2]^{2+}$ were readily formed and no isomerization of the compounds was observed under the refluxing reaction conditions using a water/acetone mixture.

In Figure 1 the ^{1}H NMR spectra of **1** (top) and **2** (bottom) in $[D_6]$acetone at room temperature are shown. The difference between the two spectra is similar to what is observed

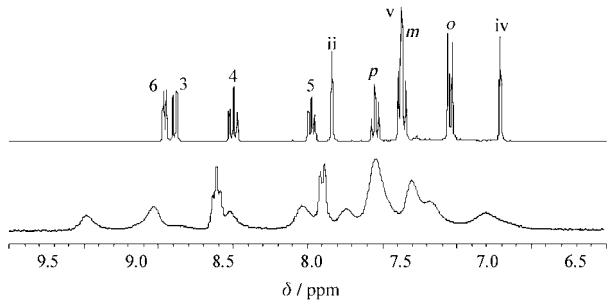

Figure 1. ^{1}H NMR spectra of **1** (top) and **2** (bottom) in $[D_6]$acetone at room temperature.

in the analogous *cis*-$[Ru(bpy)_2(L)_2](PF_6)_2$ complexes[31,32] and β-$[Ru(azpy)_2(L)_2](PF_6)_2$ complexes.[48] The bis(MeIm) adduct **1** shows well-resolved resonances, suggesting the MeIm ligands are rotating quickly around the Ru–N(iii) axes on the NMR timescale. The ^{1}H NMR spectrum of the bis(MeBim) adduct **2** on the other hand shows broad peaks, suggesting hindered rotational behavior of the MeBim ligands. From the study on *cis*-$[Ru(bpy)_2(MeBim)_2](PF_6)_2$, it is known that the two MeBim ligands coordinated to the ruthenium(II)–bis(bpy) moiety prefer specific orientations on the ruthenium giving rise to different atropisomers, observable at low temperatures.[31,32] Also, for the β-$[Ru(azpy)_2(MeBim)_2](PF_6)_2$ complex, broadening of the ligand ^{1}H NMR signals was observed with VT measurements, but only one conformer is present at low temperatures.[48]

Conformers: For two *cis*-coordinated lopsided ligands on a metal, the corresponding atoms can be on the same side (head-to-head, HH) or on opposite sides (head-to-tail, HT) of the ligand–metal–ligand plane.[18] As a lopsided ligand will preferably not orient in-plane with one of the coordination planes,[14] four staggered orientations are possible; in a "*cis*-bis" octahedral six-coordinate complex therefore, 16 conformers can be designed (Supporting Information, Figure S2). Rationalizing further, the monodentate ligands will orient with the head-to-tail axis of the heterocyclic ligands in a "parallel" fashion rather than an "orthogonal" orientation ("parallel" and "orthogonal" as in the projection used in Scheme 3 and Figure S2), as in the latter case there

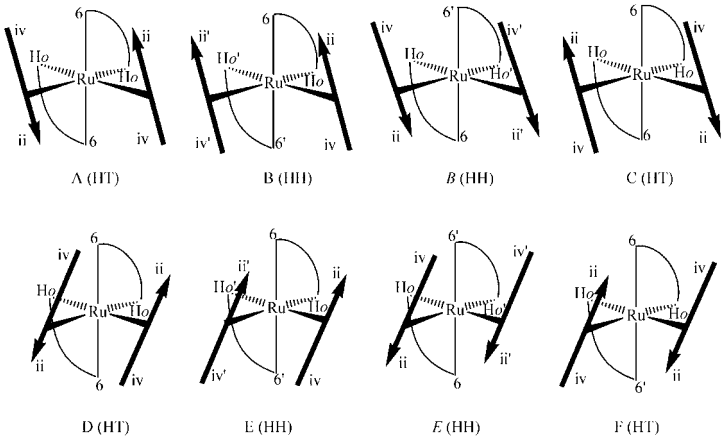

Scheme 3. Eight (six different) possible conformers of (the Λ enantiomer of) an α-$[Ru(azpy)_2(L)_2]^{2+}$ complex (the cation charge is not depicted for clarity reasons). The four (three different) atropisomers, A–C, are found in the related *cis*-$[Ru(bpy)_2(MeBim)_2]^{2+}$ complex, too.[31,32] In addition, for **2** the atropisomers D and E/*E* are also observed. The orientation of the MeBim ligands in β-$[Ru(azpy)_2(MeBim)_2]^{2+}$ (an isomer that lacks C_2 symmetry due to the inverted coordination of one of the azpy ligands, and so all eight conformers are different) is analogous to D.[48]

are severe clashes between the two *cis*-coordinated ligands and the didentate ligands. Therefore, the amount of conformers diminishes to eight: four HT and four HH isomers. Finally, due to the two-fold symmetry in the α-$[Ru(azpy)_2]$ moiety, in α-$[Ru(azpy)_2(L)_2]^{2+}$ complexes the HH isomers are two sets of identical pairs (B/*B* and E/*E*), and the number of geometrically different possible combinations of orientations of the two lopsided ligands is reduced to six (A–F, Scheme 3).

Most convenient for the first discrimination and identification of atropisomers in α-$[Ru(azpy)_2(L)_2]$ complexes is the fact that all four HT conformers have C_2 symmetry, resulting in the two azpy and the two heterocyclic monodentate ligands being indistinguishable with ^{1}H NMR spectroscopy; the two HH rotamers on the other hand lack C_2 symmetry, yielding twice as many signals with respect to an HT conformer. The two benzimidazole ligands in *cis*-$[Ru(bpy)_2(MeBim)_2](PF_6)_2$ both orient preferentially in only two different ways on the ruthenium (i.e., with the lopsided parts of the MeBim ligands, represented by the rods with the H(ii) and H(iv) sites in Scheme 3, wedged in between the didentate ligands) resulting in four (three different) atropisomers: two

HT conformers (A and C), and two "identical" HH conformers (B and *B*).[31,32] The other atropisomers depicted in Scheme 3, D–F, in which the MeBim ligands are oriented with the 5- or 6-membered ring above the didentate ring system, were not observed. In the complex β-$[Ru(azpy)_2(MeBim)_2](PF_6)_2$, however, such an orientation with an MeBim ligand above the didentate azpy ligand was found (atropisomer D),[48] and for the α ruthenium–bis(azpy) complexes it appears that such an orientation can also not be excluded. Therefore, the identification of the observed atropisomers of **2** in ^{1}H NMR experiments requires a detailed investigation and consideration of all eight conformers depicted in Scheme 3.

α-$[Ru(azpy)_2(MeIm)_2](PF_6)_2$, 1: In the aromatic region of the ^{1}H NMR spectrum of α-$[Ru(azpy)_2(MeIm)_2](PF_6)_2$ at room temperature (Figure 1), ten resonances are observed (the assignment of the signals is given in Figure 1 and in Table 1). The doublet and triplet peaks with double intensity

Table 1. Selection of ^{1}H NMR data [ppm] in [D$_6$]acetone of **1**[a] and **2**[b].

	H3	H4	H5	H6	H(*o*)	H(*m*)	H(*p*)	H(ii)	H(iv)
1	8.84	8.50	7.98	8.98	7.04	7.38	7.55	7.83	6.69
2	8.88	8.44	7.84	9.12	7.10	7.44	7.53	8.11	6.63

[a] At room temperature. [b] At 65 °C.

with respect to the other signals can directly be attributed to the azpy *ortho*, H(*o*), and *meta*, H(*m*), protons of the phenyl ring, respectively, after which a COSY spectrum readily reveals the triplet at 7.55 ppm to correspond to *para*, H(*p*). The MeIm peaks have been assigned by starting with a NOESY spectrum in which the Me(i) group is shown to interact with H(ii) as well as H(v), and the latter furthermore also shows a cross peak with H(iv) (Figure 2). Using a COSY spectrum, the four signals of the pyridine of the azpy ligands have been assigned; on the basis of the ^3J coupling, the doublet at 8.95 ppm ($^3J \sim 6$ Hz) is assigned to H6 and the doublet at 8.89 ppm ($^3J \sim 9$ Hz) to H3. This attribution is further confirmed by the (weak) inter-ligand NOE cross peak observed between the H6 and the H(*o*) resonances, which is as expected for the α-$[Ru(azpy)_2]$ isomer.[38,44,45]

The ^{1}H NMR spectrum of **1** shows one set of azpy and one set of imidazole signals, indicating a two-fold symmetry is present in the complex. In theory, from such a spectrum it is impossible to conclude whether the ligands are rotating fast or slow at the NMR timescale: one set of peaks for the two imidazole ligands and one set for the two azpy ligands can indicate the presence in solution of one C_2-symmetric (HT) atropisomer or on the other hand it can indicate a dynamic system which is in fast exchange on the NMR timescale. In *cis*-bisadducts of square-planar four-coordinate Pt^{II} complexes with guanine derivatives, this phenomenon has been nominated the "dynamic motion problem", and to solve this problem Pt^{II} complexes with large (backbone) ligand systems have been designed to increase the steric hindrance and lower the rotation speed of the ligands.[16,17,53]

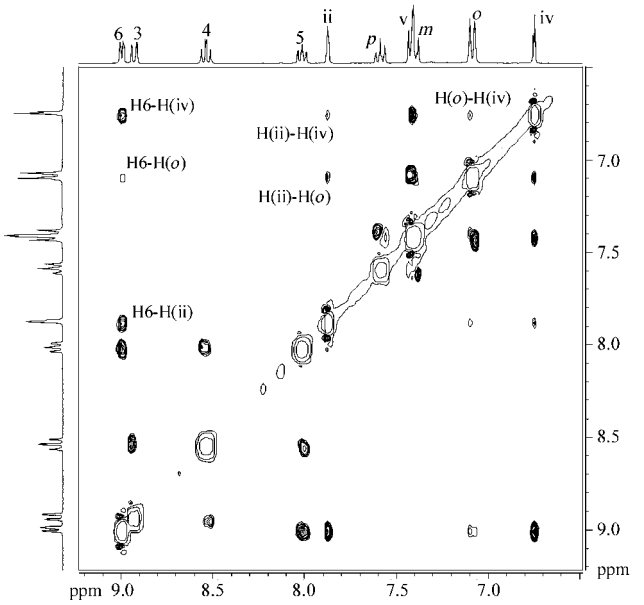

Figure 2. NOESY spectrum of **1** in [D$_6$]acetone at room temperature. The inter-ligand NOE cross peaks of the imidazole H(ii) and H(iv), and the azpy H6 and H(*o*) resonances are labeled.

The dynamic motion problem of **1** is actually addressed by changing the sterical aspects of the (rotating) ligands instead of changing the ligand backbone, that is, by comparison of the data of **1** and **2.** As the MeBim ligands in **2** are rotating rapidly around their Ru–N axes when just above room temperature, vide infra, it is reasonable to assume the smaller MeIm ligands also do so at this temperature. In the whole temperature range between 55 and −95 °C, the ^{1}H NMR spectrum of **1** does not change, indicating that at the lower temperatures the MeIm ligands are also still rotating rapidly on the NMR timescale. This in fact has been confirmed by NOESY data.

In the study with *cis*-$[Ru(bpy)_2L_2]^{2+}$ complexes it has been pointed out that the bpy is a spectator ligand, with the "static" bpy H6 and H12 protons functioning as probe protons able to monitor the orientation and the rotation of the monodentate ligands, L.[31–33,44] The NOESY results presented below indicate that, similarly, the H6 and, to a lesser extent also the H(*o*), protons of the azpy ligand can function as probe protons to monitor the orientation and rotation of *cis*-bis-coordinated ligands. The NOESY spectrum of **1** (Figure 2) shows that both the azpy H6 and the H(*o*) proton resonances interact with those of H(ii) as well as H(iv) of the MeIm ligands. There is no HT conformer depicted in Scheme 3 for which all these cross peaks can be expected. The only conformer in which H(ii) and H(iv) are expected to show interactions with the H6 and the H(*o*) protons is the HH conformer B/*B*, however, because of the lack of C_2 symmetry, twice as many resonances are expected to be seen for such a conformer. So the NOESY data confirm that the MeIm ligands in **1** are rotating (fast) on the NMR timescale around their Ru–N(iii) axes.

α-[Ru(azpy)$_2$(MeBim)$_2$](PF$_6$)$_2$, 2: The ^{1}H NMR data of **2** show a strong temperature dependence, like that observed for the related complex *cis*-[Ru(bpy)$_2$(MeBim)$_2$](PF$_6$)$_2$, showing atropisomerization on the NMR timescale.[31,32] However, significant differences and some very remarkable features are to be noted. First of all, the freezing out of the atropisomers of **2** occurs in three well-observable steps, an as yet unprecedented phenomenon for rotational behavior of metal-coordinated molecules. Second, the total number of atropisomers observed in the low-temperature ^{1}H NMR spectra is seven (five different atropisomers, considering that the two HH conformers are both present twice, see Scheme 3); the observation of four atropisomers in *cis*-bisadducts is already rare, and a total of seven is exceptionally high. Third, identification of the solution structures of the atropisomers of **2** shows two different HH and three HT isomers. HH atropisomers with non-tethered bicyclic ligands are rarely observed, the observation of two HH rotamers in one compound is unique for mononuclear octahedral complexes. Fourth, three of the seven observed atropisomers of **2** have the MeBim ligands oriented in, for steric reasons, an unexpected way, with (one of) the imidazole rings above the aza band of the azpy ligand, suggesting some kind of electrostatic interaction to stabilize this conformer. Fifth, the temperature-dependent interconversion of the different rotamers occurs by specific pathways, indicating synchronous rotation of both heterocyclic ligands occurs at the lowest recording temperatures, rather than the single rotation of one of the ligands.

The identification of the different rotamers of **2**, and their exchange mechanism is an elaborate task, requiring the consideration of numerous data obtained from 1D and 2D ^{1}H NMR spectra recorded at different temperatures and at different magnetic field strengths. For clarity reasons, the ^{1}H NMR data given below are discussed and divided into the following sections: the assignment of the resonances signals in the high-temperature spectra and 1D variable-temperature (VT) data, identification of the proton resonances in the low-temperature spectra, determination of the orientation of the MeBim ligands in the five different conformers using 2D NOE data, the (de)shielding effects of the MeBim ligands on the other proton resonances, and the interconversion of the atropisomers at different temperatures as investigated with ROESY(EXSY) data (EXSY = exchange spectroscopy).

High-temperature ^{1}H NMR data: In the ^{1}H NMR spectrum of **2** at 65 °C (Figure 3) a total of 12 signals is observed in the downfield region; H(*m*) and H(vi) overlap but are readily identified from a COSY spectrum. All the azpy proton resonances were assigned using COSY and NOESY spectra in a similar way to that described for the related MeIm complex, **1**. In the aromatic region only one singlet is observed which can be safely attributed to the H(ii) proton of the MeBim ligand; an NOE cross peak with the methyl-group resonance Me(i) at high field confirms this assignment (data not shown). The second NOE peak of the aliphatic signal

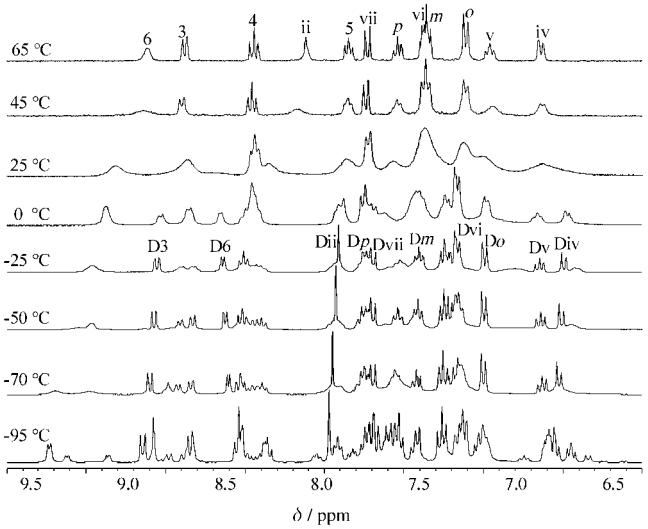

Figure 3. ^{1}H NMR spectra of **2** in [D$_6$]acetone at different temperatures. The coalesced signals at 65 °C are assigned in the figure and are listed in Table 1. A selection of relevant resonances of atropisomer D is indicated in the −25 °C spectrum. Assignments of the resonances of the different atropisomers present at −95 °C are listed in Table 2. A detailed discussion of the downfield H3/H6 region is given in Figures 4, 5, and 6.

points to the MeBim H(vii) peaks, after which the COSY spectrum consecutively reveals the H(vi), H(v), and H(iv) peaks (see discussion of **1**). In Table 1 the ^{1}H NMR data in [D$_6$]acetone of **1** (at room temperature) and **2** (at 65 °C) are listed. Interestingly, in contrast to the other signals, the H6 resonance is relatively broad at the highest measured temperature, which is due to the large frequency difference between the H6 resonances of the atropisomers when in slow exchange.

Variable-temperature ^{1}H NMR behavior: The variable-temperature (VT) behavior of **2** as studied with ^{1}H NMR spectroscopy is most peculiar (see Figure 3). As discussed above, at 65 °C one set of signals is observed and the set of pyridine and phenyl-ring resonances of the azpy ligands as well as the MeBim signals are well identified. On lowering of the temperature, the peaks start broadening, and close to room temperature, broad peaks are observed which have the aspect of coalesced signals of different atropisomers. Then, on further cooling the peaks start sharpening again and at 0 °C two sets of 12 peaks are present, "ABCE" and "D", of which the resonances have been assigned following the same procedures as described above for the high-temperature spectrum. The ratio between the peaks of the sets of signals D/ABCE is 2:3. Remarkably, on further lowering of the temperature, the resonances of the ABCE set of peaks start to broaden again whilst the resonances of D remain as well-resolved sharp signals. At −95 °C, close to the freezing point of the [D$_6$]acetone, the resonances deriving from the ABCE set of peaks are split in two sets of 12 peaks (A and C) and two sets of 24 peaks (B and E). Using the procedure described below, the NMR signals at −95 °C have been assigned to the protons of the five different atropisomers: A

(4%), B (25%), C (31%), D (37%), and E (3%). Although not all proton resonances of the two less abundant atropisomers (A and E/*E*) could be assigned due to overlap of the signals, the most relevant (i.e., the azpy H6, H6′, H(*o*), H(*o*′) and the MeBim H(ii), H(ii′), H(iv), and H(iv′) peaks) have all been determined, except for the $H(o)_A$ (see below for definition of subscript A) proton resonance (Table 2, vide infra).

Table 2. Selection of ^{1}H NMR data [ppm] of the atropisomers A, B(*B*), C, D, and E(*E*) of **2**, recorded at −95°C at 600 MHz,[a] and characteristic NOE interactions. The assignment was carried out using COSY, TOCSY, NOESY, and ROESY data from experiments at 300 and 600 MHz, and using variable mixing times for discriminating NOE and NOE–EXSY peaks. See text for detailed discussions.

	6/6	5/5′	4/4′	3/3′	*o*/*o*′	ii/ii′	iv/iv′	v/v′	vi/vi′	vii/vii′	(i)/(i′)	NOE
A	9.09	8.04	8.55	9.01	–	8.50	7.20	–	–	7.80	3.69	6-ii, 6-iv
B(*B*)	9.36	8.06	8.49	8.97	7.10	8.35	7.41	7.41	7.62	7.85	3.50	6-iv, 6-iv′, ii-iv′
	9.62	7.93	8.43	8.89	7.10	8.82	6.34	6.75	7.24	7.70	4.06	6′-ii, 6′-ii′
C	9.72	7.92	8.37	8.85	7.10	9.07	6.59	6.45	7.03	7.60	4.09	6-iv, 6-ii,
D	8.51	7.76	8.55	9.14	7.00	7.98	6.54	6.60	7.16	7.68	3.97	6-iv, ii-iv, ii-3
E(*E*)	9.12	7.92	8.40	8.78	7.20	7.60	6.12	7.15	7.48	7.94	3.80	
	9.47	8.09	8.45	8.85	7.30	7.60	6.25	7.25	7.58	7.98	3.87	

[a] As some of the atropisomers of **2** are in exchange with other atropisomers even at the lowest recording temperatures, spectra recorded at different magnetic field strengths and/or at slightly different temperatures can result in small differences in the observed resonances.

Below, the following assignment is used for identification of the proton resonances. The superscript letters indicate the averaged (coalesced) resonance peak for a specific proton of two or more atropisomers in fast exchange, whilst a subscript indicates the resonance of a proton in one specific atropisomer, for example, $H6^{ABCE}$ and $H6_A$, respectively. Note, due to symmetry reasons in the HT atropisomers of **2** the H6 and H6′ protons are indistinguishable, therefore, for example, the $H6_A$ peak corresponds to two proton resonances, that is, $H6_A$ and $H6'_A$. On the other hand, the HH atropisomers lack C_2 symmetry, and therefore the H6 and H6′ protons are distinguishable with NMR spectroscopy; however, as atropisomers B and *B* are both present, the $H6_B$ or $H6'_B$ peaks are each corresponding to two proton resonances. For the HH atropisomers B and *B* (which are identical), $H6_B$ and $H6'_B$ are used to assign the resonances of both (slowly exchanging) atropisomers, whilst $H6^B$ stands for the averaged signal of four resonances of these two atropisomers in the fast-exchange region, that is, $H6_B$, $H6'_B$, $H6_B$, and $H6'_B$. This representation is preferred to the use of $H6_{B/B}$ and $H6'_{B/B}$ and $H6^{BB}6'^{BB}$. Similarly, for the other two HH atropisomers, E and *E*, it appears more common to use E to denote both "identical" atropisomers, and only for the discussion of the mechanism of atropisomerization are these two atropisomers indicated separately, vide infra.

The VT behavior of the ^{1}H NMR signal of a specific proton in a dynamic system depends on the rate constants of the rotational processes the rotamers are involved in, and depends also on the frequency difference ($\Delta\nu$) of the proton's resonances in the different rotamers when in the slow-exchange region.[54,55] The VT behavior of the atropisomers of **2** is followed easiest via the H6 (and H6′) proton resonances in the lowfield region of the aromatic spectrum (Figures 4, 5, and 6), and in the highfield region monitoring the methyl-group resonances, vide infra (Figure 7). The pyridine rings of the azpy ligands themselves are not involved in any rotation, but their H6 protons lie close to the MeBim ligands and therefore are subject to characteristic (de)shielding effects of the two MeBim ligands in the five different atropisomers, resulting in a good dispersion of the signals. Furthermore, there is little overlap of the H6 signals with the other proton resonances.

Upon lowering the temperature from 65°C, the H6 signal of **2** at 9.12 ppm first broadens to a broad peak at 45°C, and then splits up into two well-separated peaks at 8.65 ($H6_D$) and 9.38 ppm ($H6^{ABCE}$) at 0°C (Figure 4). In the same temperature range, the H3 resonance also broadens and splits into two doublet resonances, although the frequency difference

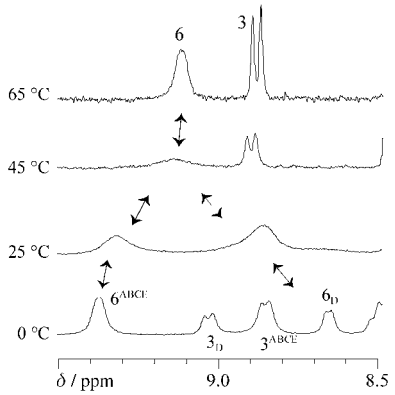

Figure 4. Enlargement of the downfield region of the VT ^{1}H NMR spectra of **2** (see Figure 3). The arrows indicate the separation of the coalesced H6 resonances at 65°C splitting into two signals at 0°C. The coalescence of the H3 peaks occurs at lower temperature than that of H6, resulting in a clear H3 doublet at 45°C, whilst H6 is not yet a well-resolved doublet even at 65°C.

between the two resonances is significantly smaller than that observed for the H6 resonances ($\Delta\nu = 54$ Hz versus 219 Hz, respectively). The frequency difference, $\Delta\nu$, of resonances of slowly exchanging protons is related to the coalescence temperature of these signals; this also explains why at higher temperatures the H3 resonance is observed as a doublet whilst the H6 signal is relatively broad, and not even completely sharpened at 65°C (see also Figure 3).

On further cooling, the lowfield peak $H6^{ABCE}$ at 9.38 ppm broadens again (−20°C) and is finally split up into six well-resolved doublets at −95°C: two sets of two doublets with equal intensity, $H6_B$, $H6'_B$ and $H6_E$, $H6'_E$, and two doublets

with different intensities, $H6_A$ and $H6_C$ (see Figure 5). Using this temperature course, in which the signal of $H6^{ABCE}$ first broadens and than separates into six signals, the $H6_D$ resonance sharpens up (−25 °C) and remains as a sharp doublet, indicating that the signal belongs to a conformer that is not involved in atropisomerization processes at these lower temperatures.

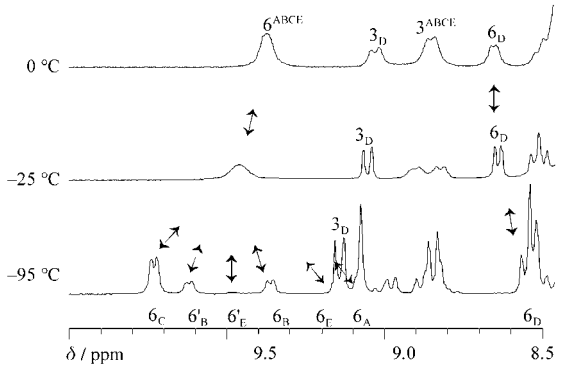

Figure 5. Enlarged part of the downfield region of VT ^{1}H NMR spectra of **2** (see Figure 3). The arrows indicate the coalesced $H6^{ABCE}$ resonance at 0 °C splitting into six doublet signals at −95 °C. The $H6_D$ resonance remains as a clear doublet on lowering of the temperature and only shows a small upfield shift.

Looking in more detail at the low-temperature course, on going down in temperature from 0 °C, the peak $H6^{ABCE}$ broadens and at −50 °C is split into a broad peak and a relatively sharp doublet, $H6^B$, (Figure 3 and Figure 6). This doublet of the $H6^B$ resonance is broadened again with lowering of the temperature and separates into two doublets of equal intensity, $H6_B$ and $H6'_B$, at −95 °C (Figure 6). The latter observation is nicely explained by a non-C_2-symmetric rotamer, that is, B, which interchanges with an identical rotamer, that is, *B* (vide infra), through synchronous rotation of both MeBim ligands by about 180°. Interestingly, this process seems to occur relatively independently from the other rotational processes in **2**, the B/*B* H6 signals showing a clear pattern, from slow to intermediate and to fast exchange. However, in NOESY and ROESY experiments recorded at −50 °C, the coalesced H6 B*B* peak also shows exchange cross peaks with other isomers, vide infra, indicating that the B/*B* isomers interconvert into other isomers, too. A rough calculation considering symmetrical and unsymmetrical two-site exchange supports the thesis of B*B* exchange as a simple two-site exchange.[56,57] Therefore, the coalescence behavior of the H6 and H6′ peaks of B/*B* illustrates a typical example of a two-site exchange of two, identical, non-C_2-symmetric atropisomers of a complex with a C_2-symmetric backbone, characterized by a double set of ligand signals (of equal intensity) with well-observable ^3J coupling, coalescing and, finally, forming one single set of averaged peaks (Figure 6), again with ^3J coupling information.

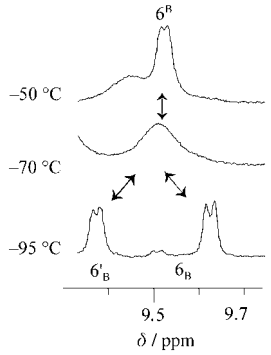

Figure 6. Close up of the VT ^{1}H NMR spectra of **2** (see Figure 3), illustrating the coalescence behavior of the two "identical" HH atropisomers B and *B*, occurring independently from other dynamic processes. The two doublet signals at −95 °C, each correspond to two proton resonances, $H6'_B/H6'_B$ and $H6_B/H6_B$, and the coalesced doublet at −50 °C, actually $H6^{BB}$, is the averaged signal of four proton resonances.

As discussed above for **1**, for **2** a single set of peaks for the two azpy ligands and one for the two MeBim ligands can also indicate the presence of only one (C_2-symmetric) conformer, or on the other hand it can indicate the average of a dynamic system which is in fast exchange on the NMR timescale. For complex **2** the ^{1}H NMR spectrum at 65 °C shows the averaged signals of different atropisomers (as deduced from the VT series), which at about 0 °C are split into two sets of peaks. At first sight these two sets of signals might be thought to belong to two C_2-symmetric atropisomers, which are in slow exchange at this temperature. Indeed one of these two sets of signals corresponds to one (HT) atropisomer, that is, D, however, the other set of peaks appears to be the coalesced signals of six (four different) other atropisomers, which are in fast exchange at 0 °C, that is, A, B(*B*), C, and E(*E*)! It is a unique occurrence that the temperature range at which the six less abundant atropisomers are in fast exchange, is the same as the temperature range at which the main atropisomer is in slow exchange. The VT ^{1}H NMR data of **2** explicitly indicate that one should take great care in interpreting the NMR data of complexes with monodentate ligands. In particular, the current study shows that for a set of signals observed in slow exchange at the NMR timescale with another set of signals, one should consider the dynamic motion problem just as for a normal ^{1}H NMR spectrum, that is, it might be a set of averaged signals of more possible atropisomers. For the H6 resonance in **2** this actually appears to occur three times upon lowering the temperature from 65 to −95 °C. In summarizing these three events, it is now useful to identify the identical HH atropisomers separately, and superscripts and subscripts indicate protons in fast- or slow-exchange, respectively. On lowering the temperature, first $H6^{ABBCDEE}$ splits up into two broad peaks, $H6^{ABBCEE}$ and $H6_D$, on further lowering of the temperature $H6^{ABBCEE}$ then separates into $H6^{BB}$, $H6_A$, $H6_C$, $H6_{EE}$, and $H6'_{EE}$, and finally $H6^{BB}$ separates into $H6'_B/H6_B$ and $H6_B/H6'_B$.

The highfield region where the Me(i) resonances are observed is also very illustrative (Figure 7). Each HT atro-

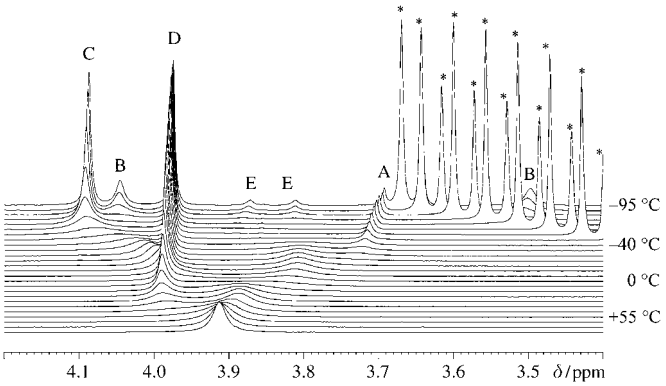

Figure 7. Highfield region of the VT ^{1}H NMR series of **2** recorded at 600 MHz, with the coalescence behavior of the Me(i) resonances of the atropisomers of **2**. Coalescence of the $Me(i)_B$/$Me(i)_B$ and $Me(i')_B$/$Me(i')_B$ signals occurs at about −40 °C. Residual solvent signals are marked (*).[58]

pisomer of **2** is expected to show one Me(i) resonance and each HH atropisomer is expected to show two, that is, Me(i) and Me(i′). In fact, at the lowest recording temperatures a total of seven resonances is present in the highfield region: two signals with high intensity ($Me(i)_C$ and $Me(i)_D$), two peaks with equal (medium) intensity ($Me(i)_B$, and $Me(i')_B$), two equally intense peaks with relatively low intensity ($Me(i)_E$ and $Me(i)'_E$), and finally one other small peak ($Me(i)_A$) close to the residual water resonance. At increasing temperature, the signals of $Me(i)_B$, and $Me(i')_B$ rapidly broaden and vanish, to finally reappear in the peak at 3.8 ppm at −40 °C, $Me(i)^B$. In the same temperature range the methyl resonances of atropisomers C and E/*E* also broaden, but the resonances of $Me(i)_A$ and $Me(i)_D$ do not broaden or shift significantly. The $Me(i)_A$ resonance starts to vanish at about −40 °C, but most particular is the $Me(i)_D$ resonance, remaining at a fixed frequency (3.98 ppm) from −95 °C up to almost room temperature, before starting to broaden significantly and shift to higher field. Above room temperature all signals coalesce into one single peak, $Me(i)^{ABCDE}$ at 3.89 ppm, at 55 °C. The highfield VT series perfectly corroborate the exchange mechanism proposed on the basis of the H6 resonances as well as that of the 2D experiments.

Proton assignment of the different atropisomers: In the aromatic region of the ^{1}H NMR spectrum of **2** at −95 °C, two sets of 12 peaks can be relatively easily distinguished and have been assigned to the atropisomers C and D. Atropisomer D is assigned to the set of peaks which do not change significantly on going down in temperature from 0 to −95 °C and are therefore readily identified with the help of the VT series; the resonances belonging to atropisomer C are attributed to the second set of relatively intense signals. Besides these two sets of 12 signals, which apparently belong to C_2-symmetric (and therefore HT) rotamers, two less abundant atropisomers are present, which both have 24 signals each, indicating a non-C_2-symmetric (HH) orientation of the two MeBim ligands, B(*B*) and E(*E*). The fifth set of signals shows only one set of resonances for each azpy and MeBim ligand (A), pointing to an HT orientation of the MeBim ligands. So, in the range of less than 4 ppm in the aromatic region of the spectrum, a total of 84 signals (7 singlets, 35 doublets, and 42 triplets) is present, requiring high resolution 2D NMR spectroscopy (see Figure 8) to identify the signals (also see the Experimental Section).

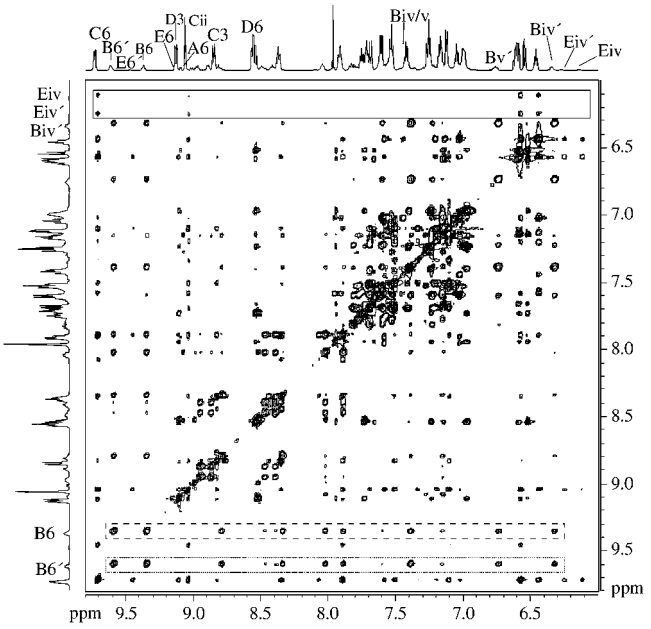

Figure 8. Aromatic region of a (600 MHz) NOESY spectrum of **2**, recorded at −95 °C. NOE and EXSY peaks have the same sign and are both shown. The H6 resonances of all atropisomers are indicated and a selection of assignments is given in Table 2. The atropisomers B and *B* being in (slow) exchange is evident from the EXSY, NOE, and NOE–EXSY peaks of B_6/$B_{6'}$ and B_6/B_6 highlighted in the dotted and dashed boxes, respectively. The exchange between atropisomer C and E/*E* is seen from the EXSY and NOE–EXSY peaks highlighted in the upper area of the spectrum.

The phenyl ring H(*o*) and H(*m*) proton signals are twice as intense as the other azpy and aromatic MeBim signals, indicating that the phenyl ring of the azpy ligand is rotating quickly around the C–N axis, as is commonly observed in ruthenium(II)–bis(azpy) complexes.[38,43,45–47] This is however not always the case, as recently shown for β-$[Ru(azpy)_2(MeBim)_2](PF_6)_2$.[44,48] For this latter complex only one conformer is observed at low temperatures, in which the stacking interaction between the phenyl ring of one azpy ligand and a MeBim ligand causes the rotation of the phenyl ring to slow down in such a way that results in two different H(*o*) and two different H(*m*) signals. From the spatial orientation of the phenyl rings in α ruthenium(II)–bis(azpy) complexes and in particular α-$[Ru(azpy)_2(MeBim)_2](PF_6)_2$, it does not seem likely that strong stacking interaction of the MeBim ligand with the phenyl ring of one of the azpy ligands can take place. The low probability for stacking interactions between

the azpy and the MeBim ligands in **2** is in fact confirmed by preliminary results of a crystallographic study of **2**.[59]

Orientations of the two MeBim ligands in the different atropisomers: The structural characterization of the five different atropisomers of **2** present in solution at −95 °C has been carried out using NOE data. The H(*o*) and H6 protons of the azpy ligands can be located close to the MeBim H(iv) or H(ii) protons in the different atropisomers, and the presence or absence of NOE interactions between these four proton resonances is used to determine the possible orientations of the MeBim ligands. The most relevant proton resonances are listed in Table 2, as well as the most important observed inter-ligand NOE cross peaks. The assignment of the five sets of peaks at −95 °C to the different atropisomers A (4%), B (25%), C (31%), D (37%), and E (3%) (see Scheme 3), is described in detail in the Supporting Information (S7). The assignment is further supported by rationalizing the characteristic (de)shielding effects on specific protons in the rotamers, as is discussed below in a separate section.

Even at the lowest recording temperature of −95 °C, some of the rotamers are in exchange (e.g., rotamer B exchanges with the identical rotamer *B*, vide infra) causing NOE data to become difficult to interpret because of NOE–EXSY peaks, due to the exchange of protons during NOE build up (see the highlighted boxes in Figure 8). Therefore, a series of spectra has been recorded with decreasing mixing time. The aromatic region of the NOESY spectrum of **2** recorded with a mixing time of 500 ms is shown in Figure 9, which in comparison with Figure 8 nicely illustrates the discrimination of NOE and NOE–EXSY peaks.

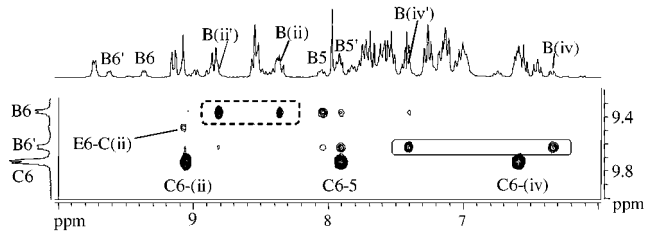

Figure 9. Part of a NOESY spectrum of **2**, recorded at −95 °C with a mixing time of 500 ms. The NOE cross peaks of $H6_B$ with the two imidazole "head" peaks $H(ii)_B/H(ii)'_B$, and of $H6'_B$ with the $H(iv)_B/H(iv)'_B$ "tail" signals are indicated with the dashed and solid lines, respectively. Some weak NOE–EXSY peaks of $H6_B$ and $H6'_B$ with the $H(ii')_B$ and $H(iv')_B$, respectively, as well as with the $H5'_B$ and $H5_B$, respectively, resonances are still visible. Rotamer E does not show any NOE cross peaks, but a NOE–EXSY peak between $H6_E$ and the $H(ii)_C$ is observed.

Taking into account that the HH rotamers B and E each represent two (identical) atropisomers, for **2**, seven out of the eight possible orientations of the two MeBim ligands, which are depicted in Scheme 3, are observed. The assignment of the sets of signals of **2** to the atropisomers A–E makes clear that the most abundant (75%) atropisomer of *cis*-$[Ru(bpy)_2(MeBim)_2](PF_6)_2$, A, that is, with the phenyl rings of the benzimidazole ligands wedged between the bpy ligands,[31,32] is only observed in a very small percentage in **2** (4%). It is most likely that the bulky, rotating, phenyl ring of an azpy ligand hinders an MeBim ligand to orient in between the pyridine of one azpy and the phenyl ring of the other azpy ligand. Interestingly, in conformer B(*B*), one of the two MeBim ligands is positioned with the six-membered ring in between the two azpy ligands, and in **2** this atropisomer is more abundant (25%) than in *cis*-$[Ru(bpy)_2(MeBim)_2](PF_6)_2$ (15%). However, the dynamic behavior of B/*B* in **2** even at the lowest recording temperatures corroborate that such an orientation is indeed not very stable. Conformer C is the second most abundant rotamer (31%) of **2** present at low temperatures; this conformer is also observed in the related *cis*-$[Ru(bpy)_2(MeBim)_2](PF_6)_2$ complex, albeit at a lower abundance (10%). A recent single-crystal X-ray diffraction study of **2** has revealed the molecular structure of atropisomer C,[59] strongly confirming the assignment based on NOE and (de)shielding data presented here. The most abundant atropisomer of **2**, D, has the MeBim ligands placed in such a way that the imidazole ring protons are oriented close to the aza bond of the respectively *fac*-coordinated azpy ligands. Besides the steric effects inhibiting easy rotation of the MeBim ligands (see Scheme 4), an electronic

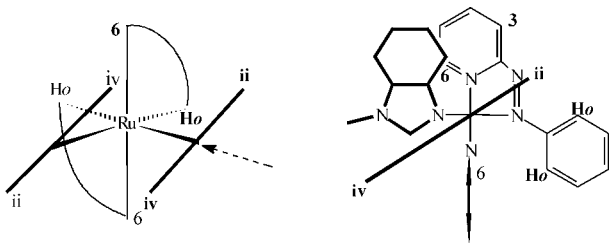

Scheme 4. Schematic representation (left) of atropisomer D of **2** (see Schemes 1–3) and projection (right) along one of the N(iii)–ruthenium axes (see dotted arrow in the left figure).

effect is possibly also stabilizing the orientations of the MeBim ligands in D. Marzilli et al.,[18] have pointed out the orientation of imidazole ligands can be partly determined by the electrostatic interaction between the positive, δ^+, side of the imidazolic CH site, and a partly negative charge (δ^-) on a neighboring ligand, like a chloride ion. In complex **2** such an interaction might be present between the imidazole ring of the MeBim ligands and the aza bond of the azpy ligands. An observation strengthening this hypothesis derives from our study on β-$[Ru(azpy)_2(MeBim)_2](PF_6)_2$,[44,48] for which at low temperatures only the conformer analogous to D is observed, and both MeBim ligands are oriented with their imidazole site close above an aza bond. The fourth possible HT conformer, F, in which the phenyl rings are oriented above the aza bond of an azpy and the H(ii) proton pointed along the pyridine ring, is not observed for **2** and this is most likely due to the sterical hindrance of the phenyl ring of the MeBim ligands with the azpy ligand. In fact, space-filling

models indicate this orientation to be quite unstable. Such an orientation of an MeBim ligand is nevertheless found in the least abundant HH rotamer, E, which is interconverting to other rotamers even at the lowest recording temperatures, indicating that the rotamer is not very stable.

Characteristic (de)shielding effects: Although the H(ii) and H(iv) protons of the MeBim ligands do show characteristic shifts in some of the rotamers, the most informative proton resonances for discriminating between all the possible atropisomers appear to be the azpy H6 signals, which are found at low field well separated from the other signals (Table 2). The H6 resonances are significantly influenced by the (presence or absence of the) shielding effect of the phenyl ring of one of the benzimidazole ligands and the deshielding effect of the other benzimidazole ligand. The (de)shielding effects of the *cis*-bis(MeBim) ligands on the H6 and H6′ protons have been discussed in detail for atropisomers A–C in the related complex *cis*-$[Ru(bpy)_2(MeBim)_2](PF_6)_2$,[31,32] and this discussion appears to be valid for the atropisomers of **2**, as well. A detailed discussion of the (de)shielding effects is given in the Supporting Information (S8).

A characteristic feature of HH atropisomers in *cis*-bis-adducts of square-planar platinum,[16] as well as octahedral ruthenium complexes,[18,24] is the lopsided ligands causing one proton resonance (H8 in guanine, H(ii) in benzimidazoles) to shift up field, and the other one down field. This is indeed also observed for the imidazole protons $H(ii)_B$ and $H(ii')_B$, for the methyl-group resonances, $Me(i)_B$ at 3.49 and $Me(i')_B$ at 4.04 ppm, and is paralleled, and even more pronounced, for the H(iv)/H(iv′) protons. In *cis*-bis-coordinated guanine–platinum complexes the characteristic guanine H8 resonances are usually discussed with respect to the mutual shielding effects of the *cis*-coordinated guanine.[60] The NMR discussion on the H(ii) resonances of the HH atropisomer B prove this is valid also for complex **2**. However, in the sterically crowded octahedral six-coordinate complexes, the (de)shielding effects of the encumbered (aromatic) didentate ligands might well contribute more than the mutual shielding of the monodentate ligands themselves. In fact, for the azpy and bpy complexes it seems more appropriate to focus on specific probe protons, for example, H6, on the static didentate ligands, in order to monitor the orientation and rotational behavior of the rotating monodentate ligands.

Exchange mechanism: The complex multi-site exchange system of *cis*-$[Ru(LL)_2(MeBim)_2](PF_6)_2$ complexes (LL is bpy or azpy) makes a quantitative analyses of the atropisomerization processes difficult; qualitatively, however, the 1D and 2D NMR data reveal much of the mechanism of atropisomerization of the dynamic system. In the *cis*-$[Ru(bpy)_2(MeBim)_2](PF_6)_2$ system it has been observed that at −95 °C, no exchange occurs between the three different atropisomers A, B, and C, whilst at slightly higher temperature, the interconversion of the two HT rotamers with the HH rotamer is observed (A⇄B and B⇄C). The lack of exchange cross peaks between the two HT atropisomers (A and C), and between the sets of signals of the HH rotamer (B⇄*B*) further indicates that the atropisomerization in *cis*-$[Ru(bpy)_2(MeBim)_2](PF_6)_2$ occurs by a single rotation of one MeBim ligand at a time.[31,32] The exchange mechanism of the atropisomers of **2** is much more complicated and requires a step-by-step analysis of the exchange data at different temperatures and monitoring of different proton resonances. In NOESY spectra of **2** at −95 °C, the NOE and exchange cross peaks have the same sign (see Figure 3); therefore, the atropisomerization analyses have been carried out by examining the EXSY level of ROESY spectra.

In Figure 10, the exchange level of a ROESY spectrum of **2** at −95 °C is shown. EXSY cross peaks are observed between the protons of atropisomer B and *B*, and also between

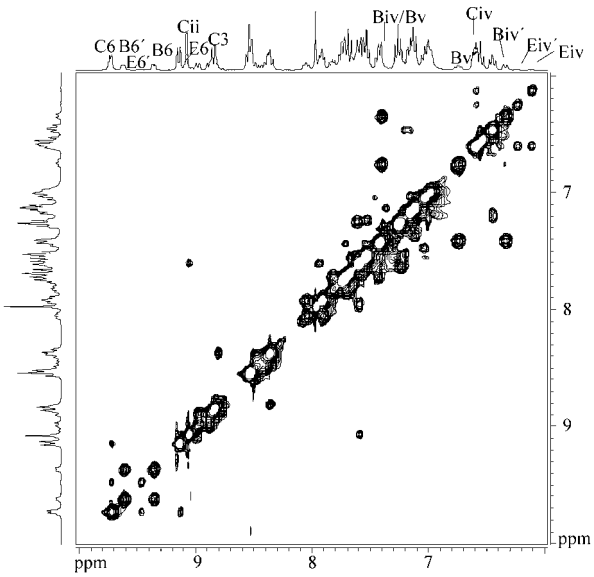

Figure 10. Aromatic region of the EXSY level of a ROESY spectrum of **2**, recorded at −95 °C with a mixing time of 500 ms. Exchange cross peaks are observed between the resonances of rotamers C and E/*E*, and between the resonances of rotamers B and *B*.

those of C and E/*E*. The resonances of rotamers A and D, on the other hand, do not show any EXSY cross peaks. Focusing on rotamer B first, the most obvious are the off-diagonal cross peaks between the protons which resonate at significantly different frequencies, like the H6/H6′, the H(ii)/H(ii′), the H(iv)/H(iv′), and H(v)/H(v′) protons (the $H(iv')_B$ and $H(v')_B$ resonances overlap at this temperature). The EXSY cross peaks between (equivalent) protons in a non-C_2-symmetric rotamer of a complex with a C_2-symmetric backbone, for example, α-$[Ru(azpy)_2]$, indicate that a rotation by about 180° of both MeBim ligands occurs, interconverting one HH rotamer into another, identical, HH rotamer (B⇄*B*, see Scheme 3). Most illustrative in this regard is also the upfield region of the spectra, where the methyl groups of the MeBim ligand resonate (see Figure 11). As no

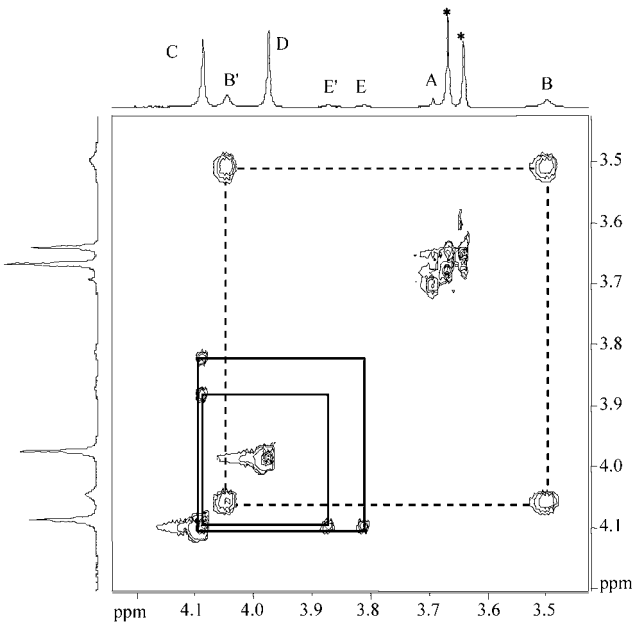

Figure 11. EXSY level of the ROESY spectrum of **2** at −95 °C. The exchange peaks between the Me(i) resonances of rotamers C and E(*E*) are indicated with solid lines, the interconversion between the rotamers B and *B* is indicated by the dashed lines. At this temperature the conformers A and D do not show any exchange cross peaks.

EXSY cross peaks from the signals of rotamer B with the resonances of rotamers A and C are observed, a step-by-step rotation in which the two MeBim ligands rotate by 180° one after the other, can be excluded. So, the atropisomer B interconverts into the identical rotamer *B* via a synchronous rotation of both MeBim ligands by about 180°. This interconversion can be understood best if the rotation of the MeBim ligand, with the six-membered rings being stacked between the pyridine and the phenyl ring, starts rotating its six-membered ring (the tail) across the *fac*-coordinated azpy ligand, and whilst it starts to rotate, it forces the second MeBim to rotate away, with the imidazole ring (the head) (see Supporting Information Figure S3).

At −95 °C, the ROESY spectrum of **2** also reveals that exchange cross peaks occur between the atropisomers C and E. Despite the overlap with other peaks, this exchange is clearly seen in the H6 region where the $H6_C$ resonance shows EXSY cross peaks with the H6 and H6′ signals of E; the H(iv) region is also illustrative, the two doublets at high field both showing cross peaks with the single $H(iv)_C$ resonance. Most informative is again the methyl region at high field (Figure 11). Different from what is observed with the other HH rotamer, B, no exchange cross peaks between the equivalent resonances of E (*E*) are observed, suggesting that simultaneous rotation of both MeBim ligands by 180° does not occur in the atropisomerization pathway of this rotamer (see Supporting Information, S9, for a more detailed discussion). For the interconversion of C into E(*E*), both MeBim ligands do have to rotate, however this requires a rotation of only 90°. The MeBim E(ii′–iv′) has to rotate 90° clockwise, whilst the second MeBim (E(ii–iv)) has to rotate 90° anti-clockwise, to result in the interconversion of E into C (see Supporting Information).[61] From a molecular model, the rotation in this way is, for steric reasons, more likely to occur than the other three possible pathways, that is, rotation of both MeBim ligands clockwise, both anti-clock wise, or both MeBim ligands rotating by 270° (the E(ii–iv) clockwise and the E(ii′–iv′) anticlockwise). Whereas the VT and EXSY data unambiguously prove the presence in solution of B as well as *B*, for E and *E* this cannot directly be concluded from the NMR spectra, as no exchange between these two "identical" HH atropisomers is observed. However, for symmetry reasons, the interconversion of C with E is energetically identical to the interconversion of C with *E*, so one can conclude that both E and *E* are present in solution and equally abundant.

In Figure 12 the downfield region of the ROESY spectra (EXSY level) of **2** is shown, recorded at −95 °C, −70 °C, −50 °C, and 0 °C. The H6 and H3 data are most informative for understanding the rotational behavior of the MeBim ligands in the seven atropisomers. As discussed above, at −95 °C, only EXSY cross peaks are observed between the (H6 resonances of) rotamers C and E/*E*, and between the two (identical) rotamers B and *B*. The observations are in perfect agreement with what is observed at high field (see Figure 11).

At −70 °C the ROESY spectrum (Figure 12) shows exchange cross peaks between the coalesced $H6^B$ resonances and the broadened $H6_C$ signal. Furthermore, rotamer A shows a strong cross peak with the broad signal of the coalesced resonances of the $H6^B$ protons. The absence of cross peaks between the $H6_D$ resonance with any of the other H6 signals is also evident, indicating that at this temperature the MeBim ligands in atropisomer D are not (or very slowly) rotating around their Ru–N axes. At this temperature, the H3 region is also very illustrative, showing the exchange cross peaks between the $H3_C/H3_E3'_E$ peaks, the coalesced $H3^B$ peaks, and the $H3_A$ signal, but not with the $H3_D$ peak.

At −50 °C the $H6_B$ and $H6'_B$ resonances are in their fast-exchange region and show one relatively sharp doublet, $H6^B$ at 9.4 ppm, whilst the H6 resonances of rotamers C and E are severely broadened. The $H6^B$ peak shows a strong EXSY cross peak with the $H6_D$ and $H6_A$ doublets. In the H3 region, the coalesced $H3_C$ and $H3_E$ resonances, $H3^{CE\mathit{E}}$, show a clear interaction with $H3^{B\mathit{B}}$ and also with $H3_D$. Between A and D, however, no exchange cross peaks are observed. This is the lowest temperature at which rotamer D clearly shows interconversion into other atropisomers.

Finally at 0 °C, the H6 resonances of A, B/*B*, C, and E/*E* are in their fast-exchange region and show one (broad) doublet at 9.35 ppm, $H6^{AB\mathit{B}CE\mathit{E}}$, which shows a strong cross peak with the $H6_D$ resonance. At this temperature, the H3 resonances of A, B, *B*, C, E, and *E* are also in their fast-exchange region and show a doublet at 8.7 ppm, which results in an exchange peak with the $H3_D$ signal at 9.0 ppm. Knowing the origin of the $H6^{AB\mathit{B}CE\mathit{E}}$ and the $H3^{AB\mathit{B}CE\mathit{E}}$ signals

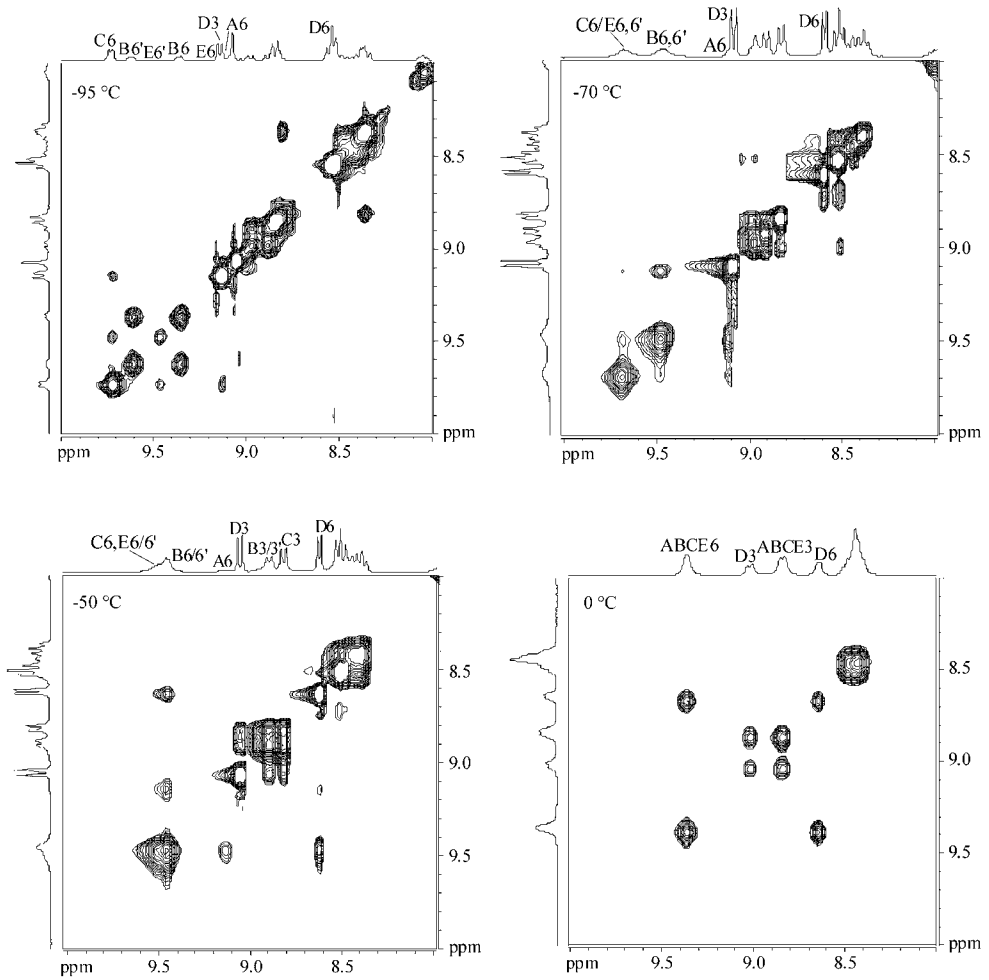

Figure 12. Downfield region of the ROESY spectra (EXSY level) of **2**, recorded at four different temperatures: At −95 °C exchange is observed between rotamers C and E(*E*) and between B and *B*; at −70 °C exchange occurs between A, B/*B*, C, and E/*E*; at −50 °C rotomer A and also D show cross peaks with coalesced signals of B/*B* and C, E/*E*; at 0 °C the H3 and H6 signals of the six rotamers A, B, *B*, C, E, and *E* are coalesced and show exchange cross peaks with the corresponding resonances of rotamer D.

from the lower temperature NMR data, this spectrum shows the unique situation in which one atropisomer is in slow exchange with six other atropisomers, which themselves are rapidly interconverting on the NMR timescale.

The NOESY spectrum of **2** at −10 °C is remarkable (see Supporting Information Figure S6) and most useful for the assignment of the signals of rotamer D. The resonances of D are sharp and show scalar and through-space cross peaks with *J* coupling information. The coalesced resonances of rotamers A, B/*B*, C, and E/*E* on the other hand are very broad and only broad NOE cross peaks are observed. The EXSY cross peaks are a hybrid between the broad and the well-resolved cross peaks.

Considering the EXSY data obtained at different temperatures, the scheme for the atropisomerization of **2** based on the 1D VT series can be extended. At the lowest recording temperature atropisomerization between B and *B* is observed, as well as between C and E/*E*. At slightly higher temperatures, interconversion between C, B/*B*, and E/*E* is also observed, as well as between A and B, but not yet between D and one of the other rotamers. The latter occurs only at higher temperatures (> −50 °C). The pathways of exchange between the rotamers have not been quantitatively identified, but it is clear that the orientation of a MeBim ligand with the six-membered ring along the pyridine site, and with the imidazole ring above the aza bond (rotamer D), is relatively stable. In addition, it can be suggested that from such a position, the MeBim ligands will preferentially rotate in only one direction, with the six-membered ring not having to "jump" over the bulky pyridine ring.[44] An important observation is also the fact that at low temperatures the simultaneous rotation of the MeBim ligands (B⇄*B* and C⇄E/*E*) is preferred above the single rotation of only one MeBim ligand (e.g., A⇄B or B⇄C).

Thermodynamic parameters: In highly symmetric systems like *cis*-$[Ru(bpy)_2(4Pic)_2](PF_6)_2$ (4Pic is 4-picoline) in which the four observed atropisomers (A, B, *B*, and C) are identical,[33] the thermodynamic parameters of the rotation of ligands can be reasonably well calculated assuming the rate

of back and forward flipping of the ligand to be identical. The dynamic processes of all atropisomers in complex **2** cannot be simplified to allow such a precise calculation. The determination of the thermodynamic parameters of the atropisomerization processes in **2** using the VT ^{1}H NMR data is a very complicated task, as there are many (energetically) different possible pathways of interconversion for the atropisomers. However, the interconversion between B and *B* is observed relatively independently from the other dynamic processes in the temperature range between −95 °C and −65 °C.[57] For the estimation of the thermodynamic data, one can regard atropisomerization of B and *B* as a simple dynamic system with two-site mutual exchange, that is, two identical compounds interconverting into each other by the synchronous flipping of both MeBim ligands by 180°. By using the frequency difference of the $H6_B$ and $H6'_B$ proton resonances in the slow-exchange area ($\Delta\nu$), at the the coalescence temperatures (T_c) the rate constant (k_c) can be roughly estimated (102 Hz, 200 K, and 226 s^{-1}, respectively). Together with data from the H3 resonances (39 Hz, 190 K, 87 s^{-1}) and the Me(i) signals (165 Hz, 215 K, 366 s^{-1}), from the Eyring equation,[54,55,56,71] the consecutively determined free enthalpy of activation $\Delta G^{\neq}$ for the simultaneous MeBim rotation in **2**, interconverting B into *B*, is 39 kJ mol^{-1}, the free enthalpy of activation, $\Delta H^{\neq}$, is 29 kJ mol^{-1}, and the free entropy of activation, $\Delta S^{\neq}$, is −50 J K^{-1} mol^{-1}. The Arrhenius activation energy (E_A) was determined to be 31 kJ mol^{-1}. The thermodynamic values obtained from a 600 MHz VT series (see Figure 13) are

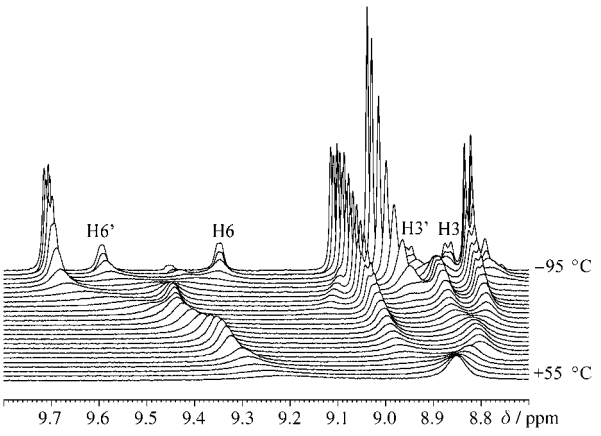

Figure 13. The downfield region of the VT NMR 1H spectra of **2** recorded at 600 MHz. In the low-temperature range the coalescence of the H6/H6′, and the H3/H3′ resonances of the atropisomers B and *B* are clearly visible. At higher temperatures the H3 resonances of all atropisomers coalesce and form a well-resolved peak at 8.85 ppm, whilst the coalesced H6 resonance is still very broad at +55 °C.

slightly different from the 300 MHz calculations ($\Delta G^{\neq}$ = 38 kJ mol^{-1}, $\Delta H^{\neq}$ = 18 kJ mol^{-1}, $\Delta S^{\neq}$ = −107 J K^{-1} mol^{-1}, and E_A = 20 kJ mol^{-1}). The differences in the parameter values as calculated from the 300 or 600 MHz data are possibly due to a relatively large error in the temperature determination.

Ligand orientation, rotation, and biological activity of ruthenium complexes: Whereas for (square-planar) platinum complexes the *cis*-bis-coordination to purines has been found to be crucial for antitumor activity, it has early been recognized that the *cis*-bis-coordination to octahedral complexes like ruthenium is sterically much more constrained.[14] Ruthenium polypyridyl complexes of the type *cis*-$[Ru(LL)_2Cl_2]$ (where LL is a didentate diimine ligand like bpy or phenantroline or, more recently, azpy) have been under investigation for their antitumor properties,[36,41] as DNA cleaving agents[39,40] as well as DNA probes[62] and appear to bind well to purines.[41,43–45] However, the bifunctional adducts of these complexes with DNA are difficult to study for stability reasons,[42] and therefore we have started to investigate the interaction of this class of compounds with DNA model bases. The *cis*-$[Ru(bpy)_2]$, α-$[Ru(azpy)_2]$, and β-$[Ru(azpy)_2]$ moieties all form stable bisadducts with MeBim and appear to be informative model compounds in the investigation of the bifunctional DNA binding of these kinds of octahedral complexes.

The results on *cis*-$[Ru(bpy)_2(L)_2](PF_6)_2$ complexes[31,32] and β-$[Ru(azpy)_2(L)_2](PF_6)_2$ complexes[44,48] together with the data on **1** and **2** presented in this paper confirm that the complexes of the type *cis*-$[Ru(LL')_2(L)_2]^{2+}$ are sterically borderline cases with respect to the ligand binding. The coordination and the orientation and rotational behavior of lopsided heterocycles in these complexes depends on relatively small differences in the ligands. The 1D and 2D VT ^{1}H NMR study presented here is a most elaborate, but very informative method to determine such small differences in sterical properties of complexes of the type *cis*-$[Ru(LL')_2]^{2+}$. The head-to-tail conformations are observed as the main conformers in all three complexes, whilst the head-to-head conformation is only present in *cis*-$[Ru(bpy)_2(L)_2](PF_6)_2$ and **2**. The HH is expected to be found in a DNA intrastrand cross-link in the major groove, the HT instead for interstrand cross-linking, in the minor groove.[40,63,64]

Whether the coordination and/or rotational properties of heterocyclic ligands to *cis*-$[Ru(LL')_2]^{2+}$-type ruthenium complexes is indeed crucial for the biological activity of the complexes is a subject that should be investigated further, using other *cis*-$[Ru(LL')_2]^{2+}$ complexes, as well as with in vitro DNA binding studies. It is now evident that coordination of the heterocyclic bidentate ligands to the bpy and the azpy complexes is significantly different.[31,32,44,48] The β-$[Ru(azpy)_2(MeBim)_2](PF_6)_2$ complex shows the presence of only one stable atropisomer, whilst the isomeric α-complex and the analogous ruthenium–bis(bpy) complex show well-defined atropisomers with specific interconversion pathways. Furthermore, the α-$[Ru(azpy)_2]^{2+}$ moiety is more versatile than the *cis*-$[Ru(bpy)_2]^{2+}$ complex: in the azpy complex more relatively stable *cis*-bisadduct orientations are possible and most of these readily interconvert into each other, furthermore there is one particularly abundant and stable isomer. The steric hindrance of the azpy ligands is likely also to promote the simultaneous rotation of both MeBim ligands. For platinum complexes it is becoming generally ac-

cepted that, besides the stable *cis*-bis(guanine) binding, the dynamic behavior of DNA binding is also crucial for antitumor activity. The octahedral ruthenium(II) complexes are on the one hand forming stable Ru–N bonds with the DNA purines, but on the other hand the sterically encumbered complexes might favor a more dynamic coordination to DNA.

Conclusion

The MeIm ligands in **1** freely rotate around their Ru^{II}–N(iii) axes, as has been concluded from VT 1D and 2D NMR studies. Compound **2** on the other hand appears to be a very remarkable complex with respect to the orientation and rotational behavior of the heterocyclic lopsided monodentate ligands. The two MeBim ligands in **2** orient in relatively stable combinations of orientations, which at low temperature have been identified as seven (five different) out of the eight (six different) theoretically possible conformers. Moreover, the exchange mechanism reveals many of the sterical properties of **2**. Two rotamers (A and D) show no exchange cross peaks with the other rotamers at low temperatures, whereas the other five rotamers, (B/*B*, C, and E/*E*) do show rotational behavior already at lower temperatures. Furthermore, the six least abundant atropisomers coalesce and are in fast exchange with each other at about 0 °C, at which it is possible to see the cross peaks between the coalesced resonances of these atropisomers, "AB*B*CE*E*", with the signals of the rotamer D. So, actually D and "AB*B*CE*E*" are in slow exchange with each other at this temperature. On lowering of the temperature, the atropisomers of **2** split stepwise into couples of atropisomers in fast or slow exchange. Most revealing is the relatively independently observed atropisomerization of the two (identical) head-to-head conformers B and *B*, allowing a rough estimation of the thermodynamic parameters of this process, which consists of the synchronous rotation of both MeBim ligands by about 180°. The synchronous rotation of both MeBim ligands appears to also be favored in the C–E/*E* atropisomerization. Overall the sterical and physicochemical properties of the α-[$Ru(azpy)_2$] backbone is such to allow the MeBim ligands in **2** to show a versatile behavior in their movements, from rocking to twisting, synchronous and not.

We started to investigate the dynamic behavior of lopsided ligands on ruthenium compounds because of their biological relevance, but the observed phenomena of ligand rotation also have interest for other fields of research. For example, the restricted rotation of parts of molecules has become an interesting subject in the investigation of molecular motors or rotors.[65,66] Octahedral six-coordinated ruthenium complexes with sterically hindered rotation of coordinated monodentate ligands might well contribute to this rising field of research.[34,35,67] In particular, complex **2** appears to be a complicated but interesting molecule showing different aspects of molecular rotation, including the synchronous rotation of two ligands, as well as temperature-dependent stepwise atropisomerization. Ruthenium(II) complexes prove to be most suitable compounds in which various aspects of ligand rotation can be investigated, tuning the physicochemical aspects of the backbone as well as the rotating ligands. In fact, for example, the observation of many atropisomers in **2** and the presence of a relatively stable isomer, D, points to ligand movements that are specific in their direction of rotation, like that observed for the ligand rotation in a monofunctional-substituted ruthenium(II)–bis(bpy) complex.[34,35] This is the subject of further research. Although we did not focus on the aspect of chirality of the conformers of **2** and other ruthenium complexes in this paper, it is of biological relevance, and furthermore is interesting for a more detailed investigation of the mechanisms of atropisomerization of these kinds of compounds.

Experimental Section

Equipment and techniques: Physical measurements were performed as described before.[32] Unless otherwise mentioned, the NMR experiments were performed at 300.13 MHz on a Bruker 300 MHz DPX spectrometer, equipped with a Bruker B-VT1000 variable-temperature unit, which was calibrated on a [D_4]methanol sample. For the 65 °C experiments, an NMR tube with sample **2** in [D_6]acetone was sealed by cautiously melting the top of the tube. Experiments at 600.13 MHz were performed on a Bruker 600 DMX spectrometer. All spectra were calibrated on the CD_3COCD_2H peak, 2.06 ppm. The 1D and 2D spectra were obtained using the standard Bruker pulse sequences. The NOESY experiments[68] were performed with variable mixing times (1 s, if not mentioned otherwise), 16 scans for each t_1 increment, and a delay of 2 s was incorporated prior to each scan. The ROESY spectra were obtained using the Bruker pulse program with a special spin lock by using a series of 180° pulses for mixing in the phase-sensitive TPPI mode.[69,70] The spin-lock field used was 2.5 kHz, and implemented for 300 or 500 ms. There were 16 scans for each t_1 increment and a 1.5 s delay was incorporated before each scan. The kinetics of atropisomerization have been studied using 1D and/or 2D NMR data.[54,55,56,71]

NMR experiments of **2** were repeated on samples obtained from different reactions and/or recrystallizations. All NMR samples showed one set of peaks at high temperatures, the same VT behavior and multiple sets of resonances at low temperatures, as described below, indicating that the latter was not due to the presence of impurities. Addition of free ligand (i.e., MeBim) to NMR samples of **2** did not change the NMR resonances of **2** at the recording temperatures, indicating that the exchange behavior was not caused by ligand-exchange phenomena.

Materials: Hydrated $RuCl_3$ was used as received from Johnson Matthey Inc. 1-Methylimidazole (Acros) and 1-methylbenzimidazole (Aldrich) were used as received. The ligand azpy,[49] and α-[$Ru(azpy)_2(NO_3)_2$],[45] were prepared according to literature procedures.

α-[$Ru(azpy)_2(MeIm)_2$](PF_6)$_2$, 1: Complex **1** was prepared by dissolving α-[$Ru(azpy)_2(NO_3)_2$] (0.20 g, 0.34 mmol) in water/acetone (1/1, 20 mL) with an excess of MeIm (0.6 g, 7 mmol), and consecutive refluxing for 6 h. After cooling down of the reaction mixture, excess NH_4PF_6 (1 g) dissolved in water (2 mL) was added, and the dark-purple precipitate formed was isolated by filtration, washed with water, and recrystallized from acetone/diethyl ether. The obtained product was recrystallized from acetone/water, and after filtration the microcrystalline residue was washed with water and dried in vacuo. Yield: 0.27 g (90 %); elemental analysis calcd (%) for $RuC_{30}H_{30}N_{10}P_2F_{12}$ ($M_r = 922\ g\,mol^{-1}$): C 39.1, H 3.28, N 15.2; found: C 39.2, H 3.30, N 15.2.

α-[$Ru(azpy)_2(MeBim)_2$](PF_6)$_2$, 2: Complex **2** was synthesized analogous to the synthesis of **1** described above, but with the use of 1-methylbenzimidazole instead of 1-methylimidazole. Yield: 0.30 g (85 %); elemental

analysis calcd (%) for $RuC_{38}H_{34}N_{10}P_2F_{12}$ ($M_r = 1021\ g\,mol^{-1}$): C 44.7, H 3.35, N 13.7; found: C 44.4, H 3.39, N 13.6.

Assignment of most resonances at the lowest recording temperature (e.g., Figure 8, a NOESY spectrum of **2** recorded at −95 °C at 600 MHz) was carried out using the following strategy: First, from the integration values in an ^1H NMR spectrum it was determined which methyl peak signals at high field, correspond with the lowfield azpy H6 doublets. Second, the methyl peaks show intra-ligand NOE cross peaks with their H(ii) and H(vii) protons, and, starting from the H(vii) peaks, the other three MeBim proton resonances were obtained consecutively from COSY and TOCSY spectra. All the H6 (and H6′) resonances were determined from the VT measurements and the exchange data, after which the other pyridine resonances were identified from the COSY and TOCSY spectra. Finally, the phenyl-ring protons of the most abundant atropisomers were assigned from the most intense cross peaks present in a COSY spectrum. The phenyl-ring H(*o*) and H(*m*) protons are twice as abundant as all the other protons, so they yield the more intense cross peaks. Where possible, the assignments have been confirmed with inter-ligand NOE cross peaks like the H(*o*)–H6 interactions. For the least abundant isomer, E, EXSY cross peaks, with the more intense C signals, have also been helpful. In Table 2, the most relevant resonances of the five rotamers A–C are listed. The attribution of the sets of signals to the different atropisomers is discussed in the text and in the Supporting Information.

Acknowledgement

C. Erkelens and A. W. M. Lefeber are kindly acknowledged for their valuable assistance with the NMR measurements. Dr. J. G. Haasnoot is thanked for reading a preliminary version of the manuscript. Johnson Matthey Inc. (Reading, UK) is acknowledged for a loan of $RuCl_3{\cdot}H_2O$. This research was sponsored by the Netherlands Council for Chemical Research, with financial aid from the Netherlands Organization for the Advancement of Research.

[1] S. J. Lippard, J. M. Berg, *Principles of Bioinorganic Chemistry*, University Science Books, Mill Valley, California, **1994**.
[2] Z. Guo, P. J. Sadler, *Angew. Chem.* **1999**, *111*, 1610; *Angew. Chem. Int. Ed.* **1999**, *38*, 1512.
[3] C. Orvig, M. J. Abrams, *Chem. Rev.* **1999**, *99*, 2201.
[4] C. X. Zhang, S. J. Lippard, *Curr. Opin. Chem. Biol.* **2003**, *7*, 481.
[5] B. Lippert, *Cisplatin*, Verlag Helvetica Chimica Acta, Zurich, Wiley-VCH, Weinheim, **1999**.
[6] J. Reedijk, *Chem. Commun.* **1996**, 801.
[7] R. E. Cramer, P. L. Dahlstrom, *J. Am. Chem. Soc.* **1979**, *101*, 3679.
[8] R. E. Cramer, P. L. Dahlstrom, *Inorg. Chem.* **1985**, *24*, 3420.
[9] A. T. M. Marcelis, H. J. Korte, B. Krebs, J. Reedijk, *Inorg. Chem.* **1982**, *21*, 4059.
[10] A. T. M. Marcelis, J. L. van der Veer, J. C. M. Zwetsloot, J. Reedijk, *Inorg. Chim. Acta* **1983**, *78*, 195.
[11] F. J. Dijt, G. W. Canters, J. H. J. den Hartog, A. T. M. Marcelis, J. Reedijk, *J. Am. Chem. Soc.* **1984**, *106*, 3644.
[12] M. D. Reily, L. G. Marzilli, *J. Am. Chem. Soc.* **1986**, *108*, 6785.
[13] Y. Xu, G. Natile, F. P. Intini, L. G. Marzilli, *J. Am. Chem. Soc.* **1990**, *112*, 8177.
[14] S. E. Sherman, D. Gibson, A. H.-J. Wand, S. J. Lippard, *J. Am. Chem. Soc.* **1988**, *110*, 7368.
[15] S. O. Ano, F. P. Intini, G. Natile, L. G. Marzilli, *Inorg. Chem.* **1999**, *38*, 2989.
[16] S. O. Ano, Z. Kuklenyik, L. G. Marzilli in *Cisplatin: Chemistry and Biochemistry of a Leading Anticancer Drug* (Ed.: B. Lippert), Verlag Helvetica Chimica Acta, Zurich, Wiley-VCH, Weinheim, **1999**.
[17] G. Colonna, N. G. Di Masi, L. G. Marzilli, G. Natile, *Inorg. Chem.* **2003**, *42*, 997.
[18] L. G. Marzilli, P. A. Marzilli, E. Alessio, *Pure Appl. Chem.* **1998**, *70*, 961.
[19] G. Sava, E. Alessio, A. Bergamo, G. Mestroni in *Topics in Biological Inorganic Chemistry*, *Vol. 1* (Eds.: M. J. Clarke, P. J. Sadler), Springer-Verlag GmbH & Co., Berlin, **1999**, p. 143.
[20] A. H. Velders, H. Kooijman, A. L. Spek, J. G. Haasnoot, D. De Vos, J. Reedijk, *Inorg. Chem.* **2000**, *39*, 2966.
[21] R. E. Morris, R. E. Aird, P. d. S. Murdoch, H. Chen, J. Cummings, N. D. Hughes, S. Parsons, A. Parkin, G. Boyd, D. I. Jodrell, P. J. Sadler, *J. Med. Chem.* **2001**, *44*, 3616.
[22] M. J. Clarke, *Coord. Chem. Rev.* **2003**, *236*, 209.
[23] A. H. Velders, A. Bergamo, E. Alessio, E. Zangrando, J. G. Haasnoot, C. Casarsa, M. Cocchietto, S. Zorzet, G. Sava, *J. Med. Chem.* **2004**, *47*, 1110.
[24] L. G. Marzilli, M. Iwamoto, E. Alessio, L. Hansen, M. Calligaris, *J. Am. Chem. Soc.* **1994**, *116*, 815.
[25] E. Alessio, L. Hansen, M. Iwamoto, L. G. Marzilli, *J. Am. Chem. Soc.* **1996**, *118*, 7593.
[26] E. Alessio, E. Zangrando, E. Iengo, M. Macchi, P. A. Marzilli, L. G. Marzilli, *Inorg. Chem.* **2000**, *39*, 294.
[27] E. Alessio, Y. H. Xu, S. Cauci, G. Mestroni, F. Quadrifoglio, P. Viglino, L. G. Marzilli, *J. Am. Chem. Soc.* **1989**, *111*, 7068.
[28] E. Alessio, M. Calligaris, M. Iwamoto, L. G. Marzilli, *Inorg. Chem.* **1996**, *35*, 2538.
[29] E. Alessio, E. Zangrando, R. Roppa, L. G. Marzilli, *Inorg. Chem.* **1998**, *37*, 2458.
[30] E. Alessio, E. Iengo, E. Zangrando, S. Geremia, P. A. Marzilli, M. Calligaris, *Eur. J. Inorg. Chem.* **2000**, 2207.
[31] A. H. Velders, A. C. G. Hotze, J. G. Haasnoot, J. Reedijk, *Inorg. Chem.* **1999**, *38*, 2762.
[32] A. H. Velders, A. C. G. Hotze, G. Van Albada, J. G. Haasnoot, J. R. Reedijk, *Inorg. Chem.* **2000**, *39*, 4073.
[33] A. H. Velders, F. Ugozzoli, C. Massera, M. Biagini-Cingi, A. M. Manotti-Lanfredi, J. G. Haasnoot, J. Reedijk, *Eur. J. Inorg. Chem.* **2002**, 193.
[34] D. Hesek, G. A. Hembury, M. G. B. Drew, V. V. Borovkov, Y. Inoue, *J. Am. Chem. Soc.* **2000**, *122*, 10236.
[35] D. Hesek, G. A. Hembury, M. G. B. Drew, V. V. Borovkov, Y. Inoue, *J. Am. Chem. Soc.* **2001**, *123*, 12232.
[36] O. Nováková, J. Kaspárková, O. Vrána, P. M. van Vliet, J. Reedijk, V. Brabec, *Biochemistry* **1995**, *34*, 12369.
[37] A. C. G. Hotze, M. Bacac, A. H. Velders, B. A. J. Jansen, H. Kooijman, A. L. Spek, J. G. Haasnoot, J. Reedijk, *J. Med. Chem.* **2003**, *46*, 1743.
[38] A. H. Velders, K. van der Schilden, A. C. G. Hotze, J. Reedijk, H. Kooijman, A. L. Spek, *Dalton Trans.* **2004**, 448.
[39] N. Grover, N. Gupta, H. H. Thorp, *J. Am. Chem. Soc.* **1992**, *114*, 3390.
[40] N. Grover, T. W. Welch, T. A. Fairley, M. Cory, H. H. Thorp, *Inorg. Chem.* **1994**, *33*, 3544.
[41] P. M. Van Vliet, J. G. Haasnoot, J. Reedijk, *Inorg. Chem.* **1994**, *33*, 1934.
[42] F. Zobi, M. Hohl, I. Zimmermann, R. Alberto, *Inorg. Chem.* **2004**, *43*, 2771.
[43] A. H. Velders, K. van der Schilden, A. C. G. Hotze, J. Reedijk, F. Ugozzoli, M. Biagini-Cingi, A. M. Manotti-Lanfredi, unpublished results.
[44] A. H. Velders, PhD Thesis, Leiden University, The Netherlands, **2000**.
[45] A. C. G. Hotze, A. H. Velders, F. Ugozzoli, M. Biagini-Cingi, A. M. Manotti-Lanfredi, J. G. Haasnoot, J. Reedijk, *Inorg. Chem.* **2000**, *39*, 3838.
[46] A. C. G. Hotze, M. E. T. Broekhuisen, A. H. Velders, H. Kooijman, A. L. Spek, J. G. Haasnoot, J. Reedijk, *J. Chem. Soc. Dalton Trans.* **2002**, 2809.
[47] A. C. G. Hotze, M. E. T. Broekhuisen, A. H. Velders, K. van der Schilden, J. G. Haasnoot, J. Reedijk, *Eur. J. Inorg. Chem.* **2002**, 369.
[48] A. H. Velders, A. Gomez-Quiroga, J. G. Haasnoot, J. Reedijk, *Eur. J. Inorg. Chem.* **2003**, 713.

[49] R. A. Krause, K. Krause, *Inorg. Chem.* **1980**, *19*, 2600.
[50] T. Bao, K. Krause, R. A. Krause, *Inorg. Chem.* **1988**, *27*, 759.
[51] S. Goswami, A. R. Chakravarty, A. Chakravorty, *Inorg. Chem.* **1981**, *20*, 2246.
[52] B. K. Santra, G. A. Thakur, P. Ghosh, A. Pramanik, G. K. Lahiri, *Inorg. Chem.* **1996**, *35*, 3050.
[53] K. M. Williams, L. Cerasino, G. Natile, L. G. Marzilli, *J. Am. Chem. Soc.* **2000**, *122*, 8021.
[54] H. Friebolin, *Basic One- and Two-Dimensional NMR Spectroscopy*, VCH, Weinheim, **1991**.
[55] J. Sandstrom, *Dynamic NMR Spectroscopy*, Academic Press, London, **1982**.
[56] P. J. Hore, *Nuclear Magnetic Resonance*, *Vol. 32*, Oxford University Press, Oxford, **1995**.
[57] The frequency difference of the H6 B/B resonances in the slow-exchange region is about 100 Hz in a 7.05 tesla field (300 MHz), indicating that in the fast-exchange region the exchange (k_{B-B}) between B and *B* is in the order of tens of kHz. At −50 °C, the (coalesced, fast-exchange) signals of isomers B and *B* show slow-exchange crosspeaks with isomer A/D, with kinetics in the order of a few Hz. So the exchange of B/*B* with other isomers is several orders of magnitude less than the B–*B* exchange.
[58] The residual water in the [D_6]acetone shows a resonance which is shifted down field on lowering the temperature, and at the lowest recording temperatures is in the region where the $Me(i)_A$ and $Me(i)_B$ resonances are found. However, at increasing temperatures, the water resonance shifts up field and the coalescence phenomena of **2** are well presented when monitoring the Me(i) signals.
[59] A. H. Velders, et.al. unpublished results.
[60] S. T. Sullivan, J. S. Saad, F. P. Fanizzi, L. G. Marzilli, *J. Am. Chem. Soc.* **2002**, *124*, 1558.
[61] The discussion regarding the direction of rotation is only valid for the Lambda enantiomeric atropisomers as depicted in Scheme 3. For the Delta atropisomers, which are indistinguishable from their mirror images in our NMR data, the direction of rotation is the opposite of what is discussed here.
[62] J. K. Barton, E. Lolis, *J. Am. Chem. Soc.* **1985**, *107*, 709.
[63] C. F. Malinge, J. M. Serre, W. Shepard, M. Roth, M. Leng, C. Zeiwer, *Nucleic Acids Res.* **1999**, *27*, 1837.
[64] H. Huang, L. Zhu, B. R. Reid, G. P. Drobny, P. B. Hopkins, *Science* **1995**, *270*, 1842.
[65] E. M. Geertsema, N. Koumura, M. K. J. ter Wiel, A. Meetsma, B. L. Feringa, *Chem. Commun.* **2002**, 2962.
[66] N. Koumura, E. M. Geertsema, M. B. van Gelder, A. Meetsma, B. L. Feringa, *J. Am. Chem. Soc.* **2002**, *124*, 5037.
[67] M. Iwamoto, E. Alessio, L. G. Marzilli, *Inorg. Chem.* **1996**, *35*, 2384.
[68] S. Macura, R. R. Ernst, *J. Mol. Phys.* **1980**, *41*, 95.
[69] T. L. Hwang, *Magn. Reson. Chem.* **1992**, *30*, S24.
[70] T. L. Hwang, *J. Am. Chem. Soc.* **1992**, *114*, 3157.
[71] C. L. Perrin, T. J. Dwyer, *Chem. Rev.* **1990**, *90*, 935.

Received: June 10, 2004
Published online: January 10, 2005